

Cosmological Constraints from High-Redshift Damped Lyman-Alpha Systems

Chung-Pei Ma¹, Edmund Bertschinger²,

Lars Hernquist³, David H. Weinberg⁵, and Neal Katz⁶

ABSTRACT

Any viable cosmological model must produce enough structure at early epochs to explain the amount of gas associated with high-redshift damped Ly α systems. We study the evolution of damped Ly α systems at redshifts $z \geq 2$ in cold dark matter (CDM) and cold+hot dark matter (CDM+HDM) models using both N -body and hydrodynamic simulations. Our approach incorporates the effects of gas dynamics, and we find that all earlier estimates which assumed that all the baryons in dark matter halos would contribute to damped Ly α absorption have overestimated the column density distribution $f(N)$ and the fraction of neutral dense gas Ω_g in damped Ly α systems. The differences are driven by ionization of hydrogen in the outskirts of galactic halos and by gaseous dissipation near the halo centers, and they tend to exacerbate the problem of late galaxy formation in CDM+HDM models. We only include systems up to the highest observed column density $N \sim 10^{21.8} \text{ cm}^{-2}$ in the estimation of Ω_g for a fair comparison with data. If the observed $f(N)$ and Ω_g inferred from a small number of confirmed and candidate absorbers are robust, the amount of gas in damped Ly α systems at high redshifts in the $\Omega_\nu = 0.2$ CDM+HDM model falls well below the observations.

Submitted to *The Astrophysical Journal Letters*

Subject headings: cosmology: theory — dark matter — galaxies: formation — hydrodynamics – quasars: general — absorption lines

¹ Department of Physics and Astronomy, University of Pennsylvania, Philadelphia, PA 19104; cpma@strad.physics.upenn.edu

²Department of Physics, Massachusetts Institute of Technology, Cambridge, MA 02139

³Presidential Faculty Fellow

⁴Department of Astronomy, University of California, Santa Cruz, CA 95064

⁵Department of Astronomy, Ohio State University, Columbus, OH 43210

⁶Department of Astronomy, University of Washington, Seattle, WA 98195

1. Introduction

High-redshift damped Ly α absorbers offer a glimpse of structure in the young Universe. These systems dominate the mass density of neutral gas in the Universe at early times and are believed to be forming galaxies (Wolfe et al. 1995; Djorgovski et al. 1996). The fraction Ω_g of the present-day critical density residing in neutral gas in these objects increases monotonically with redshift to $z \sim 3.5$ (Lanzetta, Wolfe, & Turnshek 1995; Wolfe et al. 1995). At still higher redshifts, $3.5 < z < 4.5$, recent optical spectroscopy of 27 quasars indicates a decline in Ω_g (Storrie-Lombardi et al. 1996b). This behavior is roughly what is expected in a hierarchical model of galaxy formation: a rise in Ω_g as protogalaxies are assembled, then a decline towards low redshifts as gas is converted into stars. The precise evolutionary behavior of Ω_g depends, however, on the models and can provide strong constraints on cosmological parameters when compared to the observations.

Several authors have applied the semi-analytic Press-Schechter (1974) theory for the mass function of dark matter halos to estimate Ω_g in CDM and CDM+HDM models (Mo & Miralda-Escude 1994; Kauffmann & Charlot 1994; Klypin et al. 1995). However, this analysis depends sensitively on the collapse overdensity parameter δ_c and on the assumed range of circular velocities of halos which are able to host damped Ly α systems. To reduce the uncertainties associated with this approach, Ma & Bertschinger (1994) estimated Ω_g and the column density distribution $f(N)$ of damped Ly α absorbers directly from the dark matter halos in N -body simulations. All of these studies assumed that all the gas in a dark halo becomes neutral and that the gas mass fraction in each halo is equal to the global baryon fraction. This assumption is optimistic, and therefore conservative from the point of view of ruling out cosmological models. Nonetheless, all studies found that the then-preferred $\Omega_\nu = 0.3$ version of the CDM+HDM model was ruled out by the observed abundance of damped Ly α absorbers at $z \sim 3$. Ma & Bertschinger (1994) argued that even an $\Omega_\nu \sim 0.2$ model would underpredict Ω_g by a factor of ~ 3 . With hydrodynamic simulations one can calculate the abundance and properties of damped Ly α systems directly, including the effects of gas dynamics, radiative cooling, and photoionization. The required computations are expensive and complicated, however, and so far only the standard CDM model has been studied in this way (Katz et al. 1996b, hereafter KWHM).

The goals of this *Letter* are to study the consequences of dissipation and radiative processes for damped Ly α systems in cosmological simulations and to obtain the strongest possible constraints on CDM+HDM models from the new data at $3.5 < z < 4.5$ (Storrie-Lombardi et al. 1996abc), which have yet to be considered in this context. We use the KWHM hydrodynamic simulation of standard CDM to compare $f(N)$ and Ω_g of damped Ly α systems as inferred from the gas particles directly and from the dark matter alone. The results from the CDM model are then used to calibrate our dark-matter-only, $\Omega_\nu = 0.2$, CDM+HDM simulation. This approach combines the virtues of both types of simulations and provides us with the most efficient way to obtain reliable results that incorporate gas dynamical effects without performing an expensive hydrodynamic simulation for the CDM+HDM model.

2. Simulations

The results presented here for the $\Omega_\nu = 0.2$ CDM+HDM model are based on the particle-particle-mesh (P³M) simulation reported in Ma & Bertschinger (1994) and Ma (1995). The model assumes $\Omega_{\text{cdm}} = 0.75$, $\Omega_{\text{baryon}} = 0.05$, and $h = 0.5$ ($h \equiv H_0/100 \text{ km s}^{-1} \text{ Mpc}^{-1}$). The simulation includes a total of 23 million particles (128^3 cold and 10×128^3 hot) in a cubic box of comoving sides $50 h^{-1}$ Mpc. The comoving Plummer force softening is $25 h^{-1}$ kpc, and the particle masses are $1.3 \times 10^{10} h^{-1} M_\odot$ for the cold and $3.3 \times 10^8 h^{-1} M_\odot$ for the hot particles. As shown by Ma (1995) and Fig. 1 of this *Letter*, increasing the mass resolution of the particles by a factor of ~ 10 has negligible effects on our results. The primordial power spectrum has a spectral index of $n = 1$, with density fluctuations drawn from a random Gaussian field. The normalization corresponds to the 4-year COBE rms quadrupole moment $Q_{\text{rms-PS}} = 18 \mu K$ (Bennett et al. 1996; Gorski et al. 1996), or $\sigma_8 = 0.84$ for the rms mass fluctuation in spheres of radius $8 h^{-1}$ Mpc.

The hydrodynamic simulation used here was performed with a TreeSPH code (Hernquist & Katz 1989; Katz, Weinberg, & Hernquist 1996a). We follow the evolution of structure in a conventional CDM universe with $\Omega_{\text{cdm}} = 0.95$, $\Omega_{\text{baryon}} = 0.05$, and $h = 0.5$, with the Bardeen et al. (1986) transfer function for negligible baryon density. The simulation volume is a periodic cube of comoving sides $11.1 h^{-1}$ Mpc, and it contains 64^3 gas and 64^3 CDM particles. The comoving gravitational softening length of all particles is $10 h^{-1}$ kpc. The gas and CDM particles have masses $7 \times 10^7 h^{-1} M_\odot$ and $1.4 \times 10^9 h^{-1} M_\odot$, respectively. A uniform ionizing background of $J_\nu = 10^{-22}(\nu_0/\nu)F(z) \text{ erg s}^{-1} \text{ cm}^{-2} \text{ sr}^{-1} \text{ Hz}^{-1}$ is included, where the redshift dependence $F(z)$ is taken to be unity for $2 < z < 3$, $4/(1+z)$ for $3 \leq z \leq 6$, and zero for $z > 6$. Since the metallicity of intergalactic gas at $z \gtrsim 2$ appears to be 1% or less of solar (see, e.g., Songaila & Cowie 1996 and the modeling in Haehnelt, Steinmetz, & Rauch 1996 and Hellsten et al. 1997), we use a primordial hydrogen-helium composition ($X = 0.76$, $Y = 0.24$) to compute cooling rates. The power spectrum is normalized to give $\sigma_8 = 0.7$ today. This normalization leads to roughly the observed masses of rich galaxy clusters (White, Efstathiou, & Frenk 1993), but it is nearly a factor of two below that implied by COBE (Gorski et al. 1996). Our goal here is not to investigate the validity of this model. Rather, we wish to address the general issue of the relative distribution of gas and dark matter in galactic halos and apply the results to the $\Omega_\nu = 0.2$ CDM+HDM model, which comes closer to matching simultaneously the COBE observations and the statistics of galaxies and clusters (Ma 1996).

Since we will use the KWHM TreeSPH run to calibrate the expected effects of gas dynamics in the CDM+HDM N-body run, our analysis implicitly assumes that the KWHM predictions for damped absorption in the CDM model are approximately correct, despite the finite resolution of the simulation. The physical dimensions of the damped absorbers are typically $\sim 10 - 20 h^{-1}$ kpc (see figure 2 of KWHM), significantly larger than the gravitational softening at $z \sim 3$ [$\epsilon = 10/(1+z)h^{-1}$ kpc]. It therefore seems unlikely that the overall sizes of the systems are much affected by the gravitational force softening. The cold gas in the damped absorbers is almost entirely neutral because of its high density and self-shielding, so the neutral fraction of

this component is insensitive to resolution. However, a substantial fraction of the gas in virialized objects remains hot and produces little absorption, an effect that is quite important to our results. The fraction of cooled gas can be sensitive to mass resolution in some regimes (Weinberg et al. 1997), though a hot gas fraction comparable to that in our halos is found even in 3-d and 1-d simulations with much higher resolution (Quinn et al. 1996; Thoul & Weinberg 1996; however, Navarro & Steinmetz 1997 find more efficient cooling in their simulations). The biggest uncertainty in the KWHM predictions is the inability of such simulations to model substructure on scales much smaller than the DLA systems themselves. We effectively assume that the gas distribution in damped absorbers is fairly smooth on kpc scales, whereas strong clumping could systematically shift absorption from low column densities to high column densities. Studies of DLA absorbers in gravitationally lensed quasars may eventually provide empirical constraints on the coherence of damped systems.

3. Damped Ly α Systems

The two characteristics of damped Ly α systems that we choose to examine, $f(N)$ and Ω_g , are related by $\Omega_g = H_0 c^{-1} \mu m_H \rho_{\text{crit}}^{-1} \int_{N_{\text{min}}}^{N_{\text{max}}} N f(N) dN$, where ρ_{crit} is the critical mass density today, m_H is the hydrogen mass, $\mu = 1.3$ takes into account that 24% of the mass is helium, and $N_{\text{min}} = 10^{20.3} \text{cm}^{-2}$. The upper limit to the integral could in principle be infinity, but in practice damped Ly α absorbers have been observed only up to $N_{\text{max}} \sim 10^{21.8} \text{cm}^{-2}$ (Wolfe et al. 1995; Storrie-Lombardi et al. 1996c). The absence of observed systems with higher N may reflect the small-number statistical limitations of current data, or it may indicate that at higher column densities the gas has been converted into stars. The observed $f(N)\Delta N\Delta X$ is given by the number of absorbers with HI column density in the range $N \rightarrow N + \Delta N$ in an absorption distance of $\Delta X = (1+z)^{1/2}\Delta z$ (for $q_0 = 0.5$).

The most reliable estimate of $f(N)$ in the CDM simulations comes from the gas component in the TreeSPH run. We project the gas particles in the simulation box onto a two-dimensional grid and compute the neutral hydrogen column density in each pixel. Details of the correction for self-shielding are described in KWHM. To compare with earlier work, we compute $f(N)$ from the *dark matter* component of the TreeSPH simulation by projecting each dark matter halo onto a two-dimensional grid, and converting from dark matter surface density to neutral hydrogen column density assuming a uniform ratio of neutral gas to dark matter, $\Omega_b = 0.05$, and a hydrogen baryon mass fraction $X = 0.76$. The dark halos are identified with the Denmax algorithm (Bertschinger & Gelb 1991; Frederic 1995), with no overdensity constraint imposed.

The solid and long-dashed curves in Figure 1 compare $f(N)$ at $z = 2$ obtained from the gas and dark matter components in the TreeSPH simulation. It shows a steeper slope for $f(N)$ inferred from the dark matter than from the gas, with the two curves crossing at $N \sim 10^{21.8} \text{cm}^{-2}$. The difference at the high column density end is most likely due to the cooling of the gas component, which allows it to contract to a higher density than the dissipationless dark matter, leading to a

higher $f(N)$ in Figure 1. The difference at the lower column densities could potentially reflect either different density profiles of dark matter and *total* gas in the outskirts of galactic halos, or ionization that reduces the *neutral* gas fraction in these regions (or both). To investigate the two factors separately, we computed the distribution function for the *total* hydrogen column density in the TreeSPH simulation. We found an $f(N)$ that closely matches that inferred from the dark matter at column densities $N \lesssim 10^{22} \text{cm}^{-2}$, as expected if the dark matter and the *total* gas indeed have similar density profiles outside the core of each halo. The gas and dark matter profiles in Figure 1 of Quinn et al. (1996) also support this result. Ionization therefore plays the dominant role in reducing $f(N)$. Simulations like these consistently show that cold gas lumps are embedded within halos of much hotter gas (e.g., Katz, Hernquist, & Weinberg 1992; Evrard, Summers, & Davis 1994), with little gas at intermediate temperatures. The cold gas is almost entirely neutral because of its high density and because of self-shielding. The large difference between the dark matter and gas $f(N)$ histograms at $N \sim 10^{20.5} \text{cm}^{-2}$ in Figure 1 is driven almost entirely by collisional ionization of the hot gas component.

Two other issues must be addressed before the results of Figure 1 are applied to N -body simulations of the CDM+HDM model. The first is the gravitational effect of the dense gas concentration on the dark matter in the centers of halos. The baryons, which constitute only 5% of the mass density in these models, clearly have little dynamical effect on the global clustering of the halos, but their efficient cooling in high density regions increases the depth of the gravitational potential well and can result in a higher concentration of dark matter near the halo centers in hydrodynamic simulations than in N -body runs. To quantify this effect, we performed a simulation identical to the TreeSPH run with the SPH portion turned off (i.e., a Tree run). The resulting $f(N)$ from this dark-matter-only run is shown as a short-dashed curve in Figure 1. The two histograms for the dark matter follow each other closely until $N \gtrsim 10^{21.8} \text{cm}^{-2}$, beyond which the Tree $f(N)$ falls below the TreeSPH run by more than a factor of two.

The second factor to be considered is the difference in simulation parameters between the small-box, high-resolution, hydrodynamic CDM run and the large-box, lower resolution, N -body CDM+HDM run. To bridge this gap, we compute $f(N)$ (shown as dotted curve in Fig. 1) from a P³M CDM simulation performed by Gelb & Bertschinger (1994a,b), which employed a numerical algorithm and numerical parameters similar to those of our P³M CDM+HDM run: $33 h^{-1}$ kpc for the Plummer force softening distance, $50 h^{-1}$ Mpc box, and 144^3 particles. The agreement among the various curves at $N \lesssim 10^{21.6} \text{cm}^{-2}$ is remarkable. At higher column densities, the P³M curve falls sharply, presumably because of the lower force resolution. The difference is, however, only $\sim 50\%$ up to the highest observed column densities ($N \sim 10^{21.8} \text{cm}^{-2}$), and it will be taken into account below.

Having investigated the systematic effects on $f(N)$ of dissipation, ionization, and simulation parameters in the standard CDM model, we now turn to the $\Omega_\nu = 0.2$ CDM+HDM model. Ma & Bertschinger (1994) found that $f(N)$ from the large P³M N -body simulation of this model was too steep compared to the data at $z \sim 3$, although they anticipated that ionization and gaseous

dissipation would decrease the $f(N)$ slope. Figure 1 now allows us to estimate the correction needed to “convert” dark matter to gas. We use the ratio of $f(N)$ from the gas component in the TreeSPH run (solid curve in Fig. 1) and $f(N)$ from the dark matter in the P³M run (dotted curve) as the correction factor. We multiply $f(N)$ from the CDM+HDM run by this factor for each column-density bin to correct for the effects of ionization and dissipation. The resulting $f(N)$ is shown in Figure 2 for redshifts $z = 2, 3$, and 4. Since the observed column density range extends only to $10^{21.8} \text{ cm}^{-2}$, the gas correction mainly acts to reduce $f(N)$ inferred from the dark matter and therefore worsens the problem of late galaxy formation in CDM+HDM models. There is a serious deficit of systems in the $\Omega_\nu = 0.2$ CDM+HDM model in the highest bin ($10^{21} - 10^{21.8} \text{ cm}^{-2}$) for all 3 redshifts, and a deficit for all column densities at $z = 4$. It should be noted, however, that the observed $f(N)$ are based on small numbers of systems: 12 for the redshift bin $2.5 < z < 3.5$, and 8 for $z > 3.5$ (Storrie-Lombardi et al 1996b). Moreover, some of the high-redshift systems await confirmation from high-resolution spectroscopy. If the current candidate systems are found to be blending of weaker lines, the data points will be lowered.

In the calculation above, we have assumed the same gas to dark matter conversion factor for $f(N)$ in the CDM and CDM+HDM models. Although the HDM component in the latter is less clustered than the CDM component below the neutrino free-streaming scale, we do not expect the 20% HDM present in this model to significantly alter the relation between gas and dark matter $f(N)$ in Figure 1 for the CDM model.

The neutral gas fraction in damped Ly α systems, Ω_g , is less constraining than $f(N)$, but it is still an interesting quantity to measure. Wolfe et al. (1995) find $\Omega_g = 0.0051 \pm 0.0017 h_{50}^{-1}$ at $3 < z < 3.5$, while the combined APM and Wolfe et al. sample gives $\Omega_g = 0.0030 \pm 0.0015 h_{50}^{-1}$ at $3 < z < 3.5$ and $0.0019 \pm 0.0008 h_{50}^{-1}$ at $3.5 < z < 4.7$ (Storrie-Lombardi et al. 1996b). Theoretical predictions for Ω_g depend sensitively on the upper integration limit N_{max} if the slope of $f(N)$ is flatter than -2 as observed. KWHM found the fraction of cold, dense gas in the CDM simulation to be $\Omega_g \approx 0.0065, 0.0036, \text{ and } 0.0017$ at $z = 2, 3, \text{ and } 4$, respectively. However, if we integrate $f(N)$ over the observed column density range of damped Ly α systems we find much lower Ω_g values for this model: $0.0011, 0.00096, \text{ and } 0.00069$ at $z = 2, 3, \text{ and } 4$. This drastic reduction arises because the contribution to Ω_g is dominated by the highest column density systems, which extend only to $10^{21.8} \text{ cm}^{-2}$ in the observations but to $10^{24.5} \text{ cm}^{-2}$ in the hydrodynamic simulation. To compare fairly with observations, we choose $10^{21.8} \text{ cm}^{-2}$ as the upper limit in Ω_g . When we use the gas-corrected $f(N)$ to compute Ω_g for the $\Omega_\nu = 0.2$ CDM+HDM model, we find $\Omega_g = 0.0004, 0.00025, \text{ and } 0.0002$ at $z = 2, 3, \text{ and } 4$, respectively. The values at $z = 3$ and 4 are nearly an order of magnitude below the Storrie-Lombardi et al. results. Gardner et al. (1997b) also finds deficiency in the number of damped Ly α systems in this model.

4. Discussion

In comparison to the most recent data on damped Ly α systems (Storrie-Lombardi et al. 1996abc), we find the $\Omega_\nu = 0.2$ CDM+HDM model to underpredict the column density distribution $f(N)$ of damped Ly α systems at all column densities for $z \sim 4$ and in the column density range $10^{21} \text{ cm}^{-2} < N < 10^{21.8} \text{ cm}^{-2}$ for $2 < z < 4$. Neither the CDM nor the CDM+HDM model reproduces the observed trend towards a steeper $f(N)$ at higher redshifts. We have included the effects of gaseous dissipation and ionization in our calculations by using the relative $f(N)$ from gas and dark matter in a CDM TreeSPH simulation to modify $f(N)$ from the CDM+HDM P³M run. Without considering cooling and ionization, one would obtain too steep an $f(N)$ from N -body simulations by assuming that neutral gas traces dark matter. The dark matter underpredicts $f(N)$ at higher column densities due to the lack of dissipation, and it overpredicts $f(N)$ at $N \lesssim 10^{22} \text{ cm}^{-2}$, primarily because gas ionization on the outskirts of galactic halos reduces the neutral column densities.

We have also argued that only systems up to the observed limit $N \sim 10^{21.8} \text{ cm}^{-2}$ should be included in the estimation of Ω_g for a fair comparison with data. All earlier estimates that assumed all the baryons in dark halos would contribute to damped Ly α absorption have overestimated Ω_g . The inclusion of gaseous processes therefore exacerbates the problem of late galaxy formation in all CDM+HDM models reported earlier. However, it should be remembered that the observed $f(N)$ and Ω_g are inferred from a small number of systems, some of which are yet to be confirmed by high-resolution spectroscopy.

We caution that theoretical predictions of the abundance of galactic objects at high redshifts are in general very sensitive to the normalization of the power spectrum. If the previous 2-year COBE result $Q_{\text{rms-PS}} = 20.5 \mu\text{K}$ ($\sim 1.5\sigma$ above the 4-year $18 \mu\text{K}$) is used to normalize the CDM+HDM model, the predictions in Figure 2 would be less pessimistic. However, it is generally the case that the parameter changes that would alleviate the problems of late galaxy formation in CDM+HDM (e.g., higher normalization, lower Ω_ν , $n > 1$ primeval fluctuation spectrum) would exacerbate its tendency to produce excessively massive clusters (Ma 1996).

There are certainly limitations to our numerical modeling. The hydrodynamic simulation studied in this *Letter*, for example, does not include formation of molecular clouds or stars, which would reduce the amount of atomic hydrogen available to produce damped Ly α absorption (Fall & Pei 1993; Kauffmann & Charlot 1994). However, including star formation and feedback with the simple algorithm described by Katz et al. (1996a) reduces $f(N)$ only at $N \gtrsim 10^{22.8} \text{ cm}^{-2}$ (Gardner et al. 1997a). The Ω_g obtained from systems with $10^{20.3} \text{ cm}^{-2} < N < 10^{21.8} \text{ cm}^{-2}$ therefore may not be much reduced by the process of star formation at $z \gtrsim 2$. There are additional uncertainties associated with the finite resolution of the simulations, as discussed in previous sections. The TreeSPH simulation, for example, only resolves gas cooling in halos with $v_c \gtrsim 100 \text{ km s}^{-1}$. Gardner et al. (1997a) use a combination of numerical and analytic techniques to estimate that absorption by halos with $v_c \lesssim 100 \text{ km s}^{-1}$ increases the incidence of DLA absorption in the CDM

model by about a factor of two. Unless the appropriate resolution corrections are much larger for the CDM+HDM model considered here, they will not be nearly sufficient to erase the discrepancy with the Storrie-Lombardi et al. data.

This work was supported in part by the Pittsburgh Supercomputing Center, the National Center for Supercomputing Applications (Illinois), the San Diego Supercomputing Center, NASA Theory Grants NAGW-2422, NAGW-2523, NAG5-2816, NAG5-2882, and NAG5-3111, NASA HPCC/ESS Grant NAG5-2213, NSF Grant AST 9318185, the Presidential Faculty Fellows Program, and a Caltech PMA Division Fellowship.

REFERENCES

- Bardeen, J., Bond, J. R., Kaiser, N., & Szalay, A. 1986, ApJ, 304, 15
- Bennett, C. L. et al. 1996, ApJ, 464, L1
- Bertschinger, E. & Gelb, J. M. 1991. Comput. Phys, 164
- Djorgovski, G., Pahre, M., Bechtold, J., & Elston, R. 1996, Nature, 382, 234
- Evrard, A.E., Summers, F.J. & Davis, M. 1994, ApJ, 422, 11
- Fall, S. M., & Pei, Y. C. 1993, ApJ, 402,479
- Frederic, J. 1995, ApJS, 97, 259
- Gardner, J.P., Katz, N., Hernquist, L. & Weinberg, D.H. 1997a, ApJ, in press
- Gardner, J.P., Katz, N., Weinberg, D.H. & Hernquist, L. 1997b, ApJ, submitted
- Gelb, J. M. & Bertschinger, E. 1994a, 436, 467; 1994b, 436, 491
- Gorski, K. M. et al. 1996, ApJ, 464, L11
- Haehnelt, M.G., Steinmetz, M., & Rauch, M. 1996, ApJ, 465, L65
- Hellsten, U., Davé, R., Hernquist, L., Weinberg, D. H. & Katz, N. 1997, ApJ, submitted
- Hernquist, L. & Katz, N. 1989, ApJS, 70, 419
- Katz, N., Hernquist, L., & Weinberg, D. H. 1992, 399, L109
- Katz, N., Weinberg, D. H., Hernquist, L. 1996a, ApJS, 105, 19
- Katz, N., Weinberg, D. H., Hernquist, L. & Miralda-Escude, J. 1996b, ApJ, 457, L57 (KWHM)
- Kauffmann, G., & Charlot, S. 1994, ApJ, 430, L97
- Klypin, A., Borgani, S., Holtzman, J., & Primack, J. R. 1995, 444, 1
- Lanzetta, K. M., Wolfe, A. M., & Turnshek, D. A. 1995, ApJ, 440, 435
- Ma, C.-P. 1995, in *Dark Matter*, ed. S. Holt, & C. L. Bennett (American Institute of Physics, Washington), p. 420

- Ma, C.-P. 1996, *ApJ*, 471, 13
- Ma, C.-P., & Bertschinger, E. 1994, *ApJ*, 434, L5
- Mo, H. J., & Miralda-Escude, J. 1994, *ApJ*, 430, L25
- Navarro, J. F., & Steinmetz, M. 1997, *ApJ*, 478, 13
- Press, W. H., & Schechter, P. 1974, *ApJ*, 187, 425
- Quinn, T.R., Katz, N. & Efstathiou, G. 1996, *MNRAS*, 278, L49
- Songaila, A. & Cowie, L. L. 1996, *AJ*, 112, 335
- Storrie-Lombardi, L. J., Irwin, M. J., & McMahon, R. G. 1996a, *MNRAS*, 282, 1330
- Storrie-Lombardi, L. J., McMahon, R. G., Irwin, M. J., 1996b, *MNRAS*, 293, L79
- Storrie-Lombardi, L. J., McMahon, R. G., Irwin, M. J., & Hazard, C. 1996c, *ApJ*, 468, 121
- Thoul, A.A. & Weinberg, D.H. 1996, *ApJ*, 608, 465
- Weinberg, D.H., Hernquist, L. & Katz, N. 1996, *ApJ*, in press
- White, S.D.M., Efstathiou, G., & Frenk, C.S. 1993, *MNRAS*, 262, 1023
- Wolfe, A. M., Lanzetta, K. M., Foltz, C. B., & Chaffee, F. H. 1995, *ApJ*, 454, 698

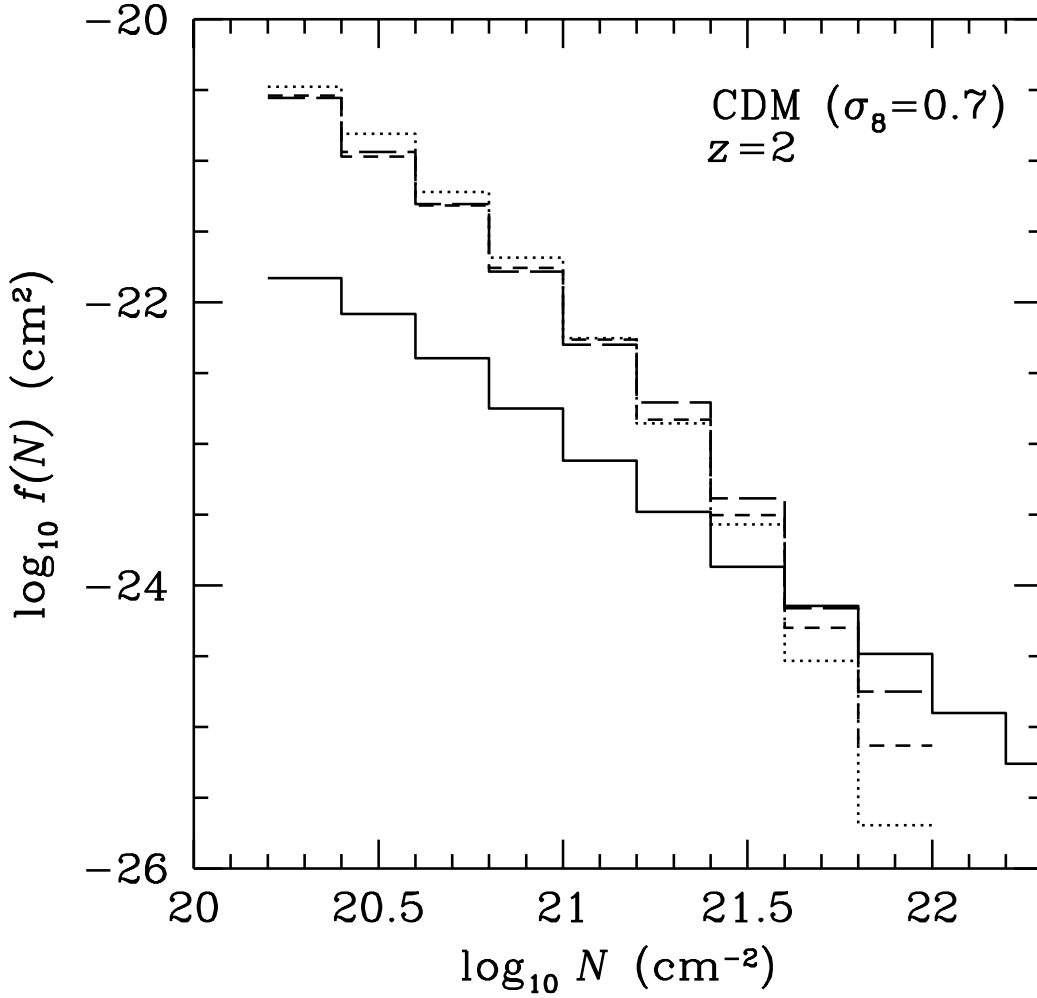


Fig. 1.— Column density distribution of damped Ly α systems at $z = 2$ in the $\sigma_8 = 0.7$ CDM model. The solid histogram is computed from the *gas* component in the TreeSPH simulation (KWHM). The long-dashed, short-dashed, and dotted histograms are computed from the *dark matter* component in a TreeSPH, Tree, and P³M simulation, respectively, under the assumption that gas and dark matter trace similar density profiles in galactic halos. The Tree run is identical to the TreeSPH with the SPH portion turned off; the P³M CDM run has similar numerical parameters as the P³M CDM+HDM run studied in this *Letter*. (See text for the exact parameters.)

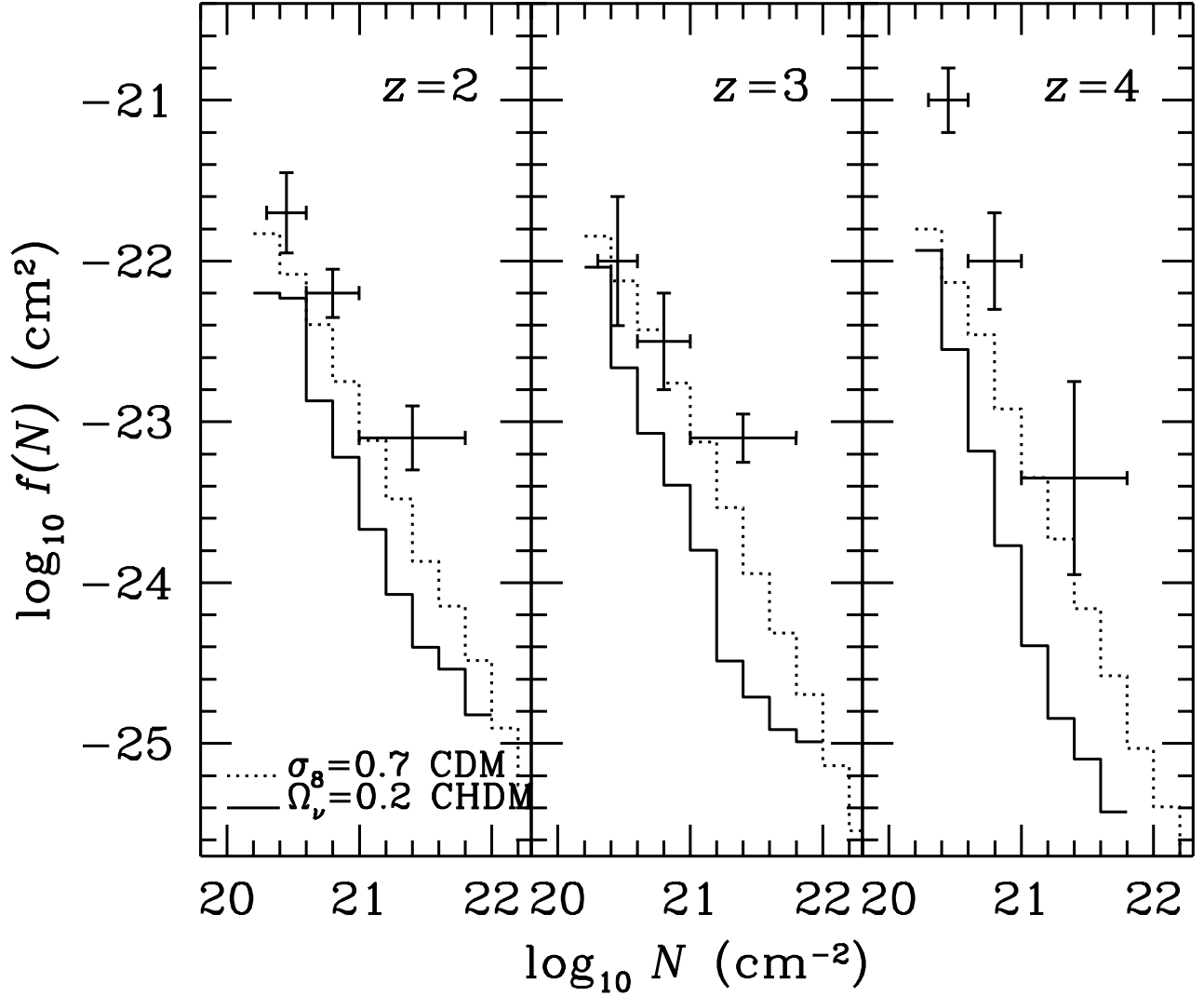


Fig. 2.— Column density distribution at $z = 2, 3,$ and 4 from observations (Storrie-Lombardi et al. 1996a) and models. The dotted histogram is computed from the gas component in a TreeSPH simulation of the low-amplitude CDM model ($\sigma_8 = 0.7$). The dashed histogram is the computed from a P^3M simulation of the $\Omega_\nu = 0.2$ CDM+HDM model normalized to the COBE $Q_{\text{rms-PS}} = 18 \mu K$, including the effects of gas dissipation and ionization.